

William S. C. Chang, Siamak Forouhar, Jean-Marc Delavaux and Ron-Xin Lu

Department of Electrical Engineering and Computer Sciences
University of California, San Diego
La Jolla, California 92093ABSTRACT

Theoretical designs of chirped grating lenses have yielded very high efficiency and moderately large angular fields of view. Experimentally, high efficiency (0.7dB insertion loss) and large angular field of view (0.1 radians) have been obtained in low index glass waveguides. Performance in high index waveguides such as LiNbO_3 will be limited by the $n_{\text{eff}}-n_s$, the index of the groove material and the tolerance of the microfabrication processes.

For signal processing in planar waveguides, it is necessary to integrate, focus, collimate, image- or Fourier-analyze guided-wave beams by efficient lenses that have both diffraction-limited performance and low noise.

Currently, the most commonly used guided-wave lens is a geodesic lens that requires the precision grinding of the non-spherical surface contour for each lens¹. Lens effect can also be obtained by diffraction from surface relief patterns made by much-less expensive planar microfabrication techniques, as illustrated in Fig. 1. Fresnel lenses have been reported to give diffraction-limited focused spot size, 10° angular field of view, and 23% efficiency at $F \geq 5^2$. An experimental linear chirped grating lens with $F = 15$ has been reported to give a diffraction-limited focused spot size with 90% efficiency³. Both of these lenses were made on low index waveguides. Optical signal processing is usually performed on electro-optical waveguides, such as LiNbO_3 , that have a high index. Questions have been raised concerning the effectiveness of diffraction lenses on high index waveguides where the index of grating grooves are limited by available materials.

We discuss in this paper the design of the chirped grating lenses in optical waveguides obtained from three types of theoretical analysis plus experimental evaluations. The design data includes (a) the efficiency η (i.e. the insertion loss), (b) the angular field of view $\Delta\theta$, (c) the spot size σ and (d) the main lobe to side lobe intensity ratio, I_0/I_s of the diffracted patterns for (1) waveguides and grooves that have different refractive indices, thicknesses and patterns and (2) lenses that have various aperture size H , F-number, focal length f and (3) incident beams that have various radiation patterns.

The theoretical design⁴ predicts that high efficiency ($\eta \approx 90\%$) can be obtained with relatively large $\Delta\theta$ ($\Delta\theta \approx 0.1$ radians) for linear chirped grating lenses that have large diffraction coupling coefficient K_c ($K_c \approx 0.05$ to 0.1) on waveguides that have an effective index n_{eff} significantly different than the refractive index of the substrate n_s . For example, Fig. 2 shows the calculated diffraction efficiency η , of a few LiNbO_3 chirped grating lenses. Notice the performance improvement that can be obtained by large coupling coefficient K_c and shape control. K_c is defined here as the change in the effective-index of the region inside and outside of the grating groove divided by half of the free space wavelength. A large coupling coefficient K_c allows us to obtain medium Q-factor lenses that will have a larger

angular field of view than the high Q-factor lenses that are typically obtained when K_c is small. Ultimately the angular field of view $\Delta\theta$ will be limited by $n_{\text{eff}}-n_{\text{substrate}}$ so that the incident beam will not be diffracted significantly into substrate modes. $\Delta\theta_{\text{max}} = \cos^{-1}(n_{\text{substrate}}/n_{\text{eff}})$. Fig. 3 shows the calculated K_c values for deposited TiO_2 film ($n = 2.57$) thicknesses (solid curves) and for various etched thicknesses in Ti-indiffused LiNbO_3 waveguides (dashed curves). Notice the importance of maintaining a mode depth δ_m of $1 \mu\text{m}$ in addition to large index for the deposited grooves for obtaining even moderately large K_c values.

Experimentally, we have investigated the deposition of CeO_2 and Nb_2O_5 films on glass waveguides by evaporation and by reactive sputtering techniques and measured changes in the effective index Δn_e of the waveguide modes created by these overlay films at various thicknesses. The measured value of Δn_e agrees approximately with theoretical predictions. Based upon the measured values of Δn_e we have fabricated CeO_2 grating lenses on glass waveguides. The mask patterns for the lenses were fabricated by electron beam lithography at the NSF National Research and Resource Center at Cornell University. The lift-off method using the conformable contact printing technique has been used successfully to fabricate the CeO_2 chirped grating fingers from these flexible Cr masks into the glass waveguides. The grating groove patterns, the length and the thickness of the experimental lenses were selected according to the theoretical design. So far the highest thru-put efficiency that has been achieved is 80% (i.e. 0.7dB total insertion loss). These lenses have a moderately large angular field of view (approximately 0.1 radians). Additional experimental investigation of constant periodicity gratings has also been carried out in order to determine the effect of (a) the Q-factor, (b) the mode polarization (i.e. TE or TM) and (c) the fabrication tolerance, on the coupling coefficient between the incident and the diffracted beams, the efficiency and the angular field of view.

Experimentally the LiNbO_3 waveguide differs considerably from glass waveguides in three aspects: (a) It has a high n_{eff} so that the material used for the grating grooves needs to have an even higher index in order to obtain large coupling coefficient at small thicknesses. (b) Its n_{eff} is very close to $n_{\text{substrate}}$ (e.g. $n_{\text{eff}} - n_{\text{substrate}} \approx 0.005$ for Ti-indiffused waveguides) so that the coupling to the substrate mode may limit either the maximum angular field of view or even the efficiency at Bragg angle. (c) The Ti

indiffused waveguide has a large mode depth caused by the small $n_{\text{eff}} - n_{\text{substrate}}$. As shown in Fig. 3, the large mode depth implies small coupling coefficient and small angular field of view.

We have investigated the deposition of TiO_2 films on LiNbO_3 waveguides. Hard, transparent and durable films of TiO_2 with refractive index close to the index of the bulk TiO_2 crystal have been obtained. TiO_2 lenses have been fabricated on Ti indiffused LiNbO_3 waveguides by a similar lift-off method as that used for the CeO_2 lenses on glass waveguides. However, due to the limitations in n_{eff} and in mode depth, the highest efficiency obtained so far is 50%. Subsequently we have investigated the use of a Nb_2O_5 transition waveguide as shown in Fig. 4 in order to obtain a larger $n_{\text{eff}} - n_{\text{sub}}$ and a higher coupling coefficient. Alternatively we have investigated the use of ion exchange in benzoic acid for obtaining the same effect. Experimental data collected up to the time of the MTT symposium on the LiNbO_3 waveguide grating lenses using these two transition waveguides will also be presented.

REFERENCES

1. Technical Digest of IEEE/OSA "Third International Conference on Integrated Optics and Optical Fiber Communication", April 27-29, 1981, San Francisco, CA.
2. W. S. C. Chang and P. R. Ashley, "Fresnel Lens in Optical Waveguides", J. Quantum Electronics, QE-16, 744 (1981).
3. S. K. Yao and D. E. Thompson, "Chirped Grating Lens for Guided-Wave Optics", Appl. Phys. Letters, 33(7), 635 (1978).
4. Z.-Q. Lin, S. T. Zhou, W. S. C. Chang, S. Forouhar and J. Delavaux, "A Generalized Two-Dimensional Coupled-Mode Analysis of Curved and Chirped Periodic Structures in Open Dielectric Waveguides", MTT Transactions, MTT-29, 881 (1981).

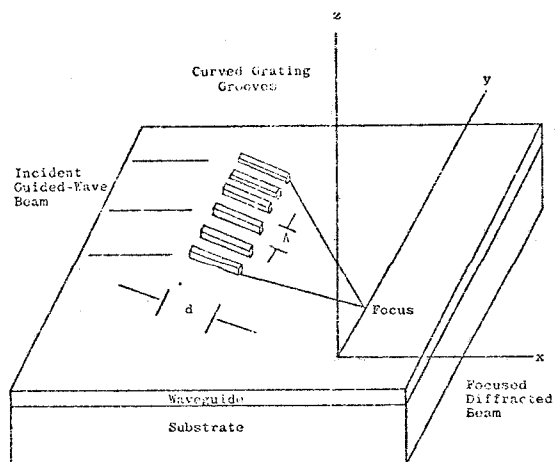


Figure 1: ILLUSTRATION OF A CURVED CHIRPED WAVEGUIDE LENS.

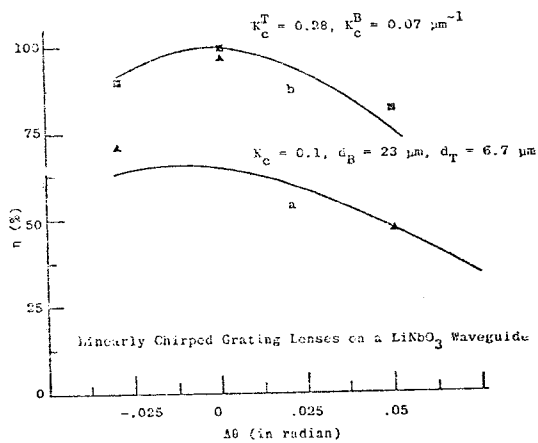


FIGURE 2: DIFFRACTION EFFICIENCY AS A FUNCTION OF THE INCIDENCE ANGLE.

Curve (a) refers to a shape controlled grating lens on LiNbO_3 waveguide with aperture $H = 2 \text{ mm}$, focus length $f = 20 \text{ mm}$, maximum groove length $d_B = 23 \mu\text{m}$, $Q = 5$, coupling coefficient $K_C = 0.1 \mu\text{m}^{-1}$.

Curve (b) refers to a grating lens with the same H , f , d_B and Q , but with a controlled K_C value, $K_C^B = 0.07 \mu\text{m}^{-1}$ and $K_C^T = 0.28 \mu\text{m}^{-1}$.

Points marked \blacktriangle refer to a rectangular grating lens with $d = 15.7 \mu\text{m}$ and $K_C = 0.1 \mu\text{m}^{-1}$.

Points marked \blacksquare refer to a rectangular grating lens with $d = 7.85 \mu\text{m}$ and $K_C = 0.2 \mu\text{m}^{-1}$.

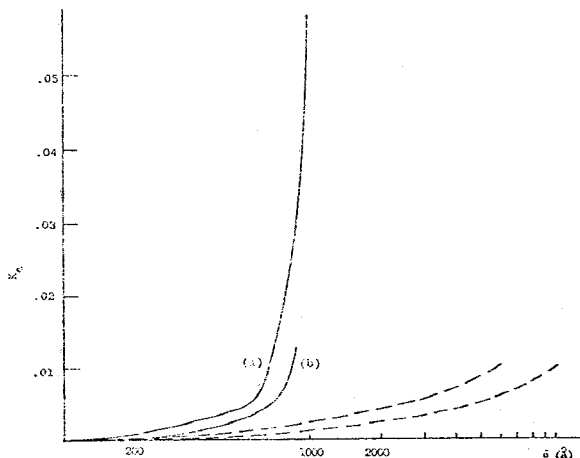


FIGURE 3: A COMPARISON OF K_C FOR ETCHED LiNbO_3 AND DEPOSITED TiO_2 GRATING GROOVES ON LiNbO_3 WAVEGUIDES.

Solid curves are the calculated K_C for TiO_2 deposited grating grooves. The dashed curves are the calculated K_C for etched grating grooves in LiNbO_3 waveguides. Curve shows only the region of single mode operation.

(a) The effective mode depth of the waveguide is 1 μm .

(b) The effective mode depth of the waveguide is 2 μm .

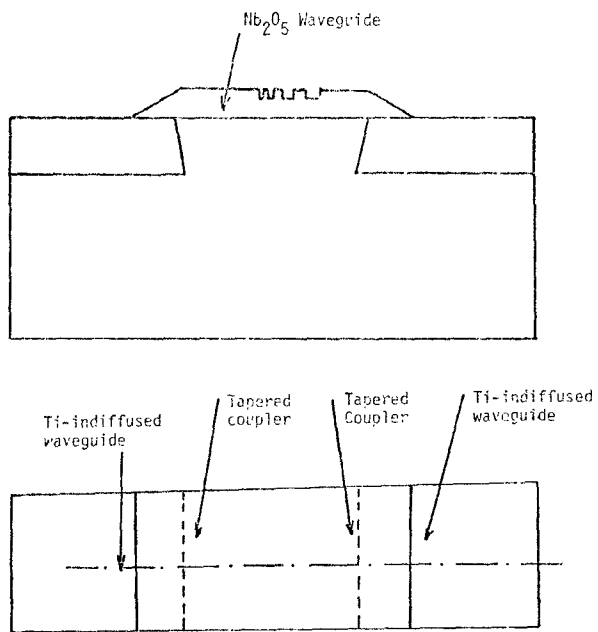


FIGURE 4: THE Nb_2O_5 TRANSITION WAVEGUIDE INTERCONNECTING
TWO SECTIONS OF A LiNbO_3 WAVEGUIDE.